Talanta 91 (2012) 18–25

Contents lists available at SciVerse ScienceDirect

Talanta

journal homepage: www.elsevier.com/locate/talanta

Thiophene anchored coumarin derivative as a turn-on fluorescent probe for Cr^{3+}: Cell imaging and speciation studies

Subarna Guha[a], Sisir Lohar[a], Arnab Banerjee[a], Animesh Sahana[a], Ipsit Hauli[b], Subhra Kanti Mukherjee[b], Jesús Sanmartín Matalobos[c,**], Debasis Das[a,*]

[a] Department of Chemistry, The University of Burdwan, Burdwan, West Bengal, India
[b] Department of Microbiology, The University of Burdwan, Burdwan, West Bengal, India
[c] Departamento de Química Inorgánica, Facultade de Química, Avda. Das Ciencias s/n, 15782 Santiago de Compostela, Spain

ARTICLE INFO

Article history:
Received 27 September 2011
Received in revised form 3 December 2011
Accepted 5 December 2011
Available online 8 December 2011

Keywords:
Thiophene–coumarin
X-ray structure
Fluorescence enhancement
Cr^{3+}
Speciation
Cell imaging

ABSTRACT

A thiophene–coumarin hybrid molecule, (6E)-6-((thiophen-2-yl)methyleneamino)-2H-chromen-2-one (**TMC**) has been prepared and its single crystal X-ray structure is reported. **TMC** can selectively detect Cr^{3+} in presence of other common cations. Both **TMC** and its Cr^{3+} complex are well characterized by different spectroscopic techniques like ^{1}H NMR, QTOF-MS ES$^+$, FTIR and elemental analysis as well. **TMC** exhibits fluorescence enhancement upon binding Cr^{3+} in CH_3CN–HEPES buffer (0.02 M, pH 7.4) (4:6, v/v) medium. Detection limit of the method is 1×10^{-6} M. Binding constant is estimated with the Benesi–Hildebrand method and the value 8×10^4 indicates a fairly strong interaction between **TMC** and Cr^{3+}. Speciation studies have been performed in a fast and environment friendly way using least sample volume, less hazardous chemicals and solvents. Cr^{3+} assisted restricted rotation around the imine bond and inhibited photo-induced electron transfer from the N,S-donor sites to the coumarin unit are responsible for fluorescence enhancement. **TMC** is capable to detect intracellular Cr^{3+} in living cells.

1. Introduction

Cr^{3+} is an essential micro nutrient for maintenance of "glucose tolerance factor" whereas excess Cr^{3+} is harmful to human health [1]. On the other hand, Cr(VI) is extremely toxic and potentially carcinogenic [2,3]. Higher oxidation potential and relatively smaller size of Cr(VI) enables it to penetrate biological cell membranes. It causes skin lesions [4], dental erosion, lung cancer and other forms of cancer [5]. Chromium compounds are used in wood preservatives and as an anti-corrosion agent [6]. General methods for measuring chromium include titrimetry [7], potentiometry [8], spectrophotometry [9–11], fluorimetry [12,13], chromatography [14], solid-phase spectrophotometry coupled to anion exchange membrane [15], flame atomic absorption spectrometry [16,17], graphite furnace atomic absorption spectrometry [18,19], inductively coupled plasma atomic emission spectroscopy [20], X-ray fluorescence spectrometry [21] and electrochemical methods [22,23].

Fluorescence method has more advantages over all the other mentioned methods due to its operational simplicity, high selectivity, sensitivity, rapidity, nondestructive methodology, enhanced sensitivity, high sampling frequency and low cost of equipment and direct visual perception [24]. For an efficient fluorescent sensor, in addition to high selectivity towards the target ion, a significant change in the fluorescence intensity and/or a spectral change of the probe are essential upon its interaction with the specific analyte [25]. Very few of the reported Cr^{3+} selective fluorescent sensors [26] have been used for trace level speciation and estimation [27]. We [28] have recently reported trace level determination and speciation of chromium using 9-acridone-4-carboxylic acid as a Cr^{3+} selective fluorescent probe.

Paramagnetic nature of Cr^{3+} limits the development of its turn-on fluorescent sensor and consequently fluorescence monitoring of intracellular Cr^{3+} in living cells remains underdeveloped. Sarkar et al. [29] reported di-(2-ethylsulfanylethyl)amine as a Cr^{3+} selective receptor in tetrahydrofuran. Mao et al. [30] reported two fluorescent sensors capable of discriminating Fe^{3+} and Cr^{3+}. 8-hydroxyquinoline containing rhodamine B derivative [31] is used for bio-imaging of Cr^{3+} in contaminated cells. Zhou et al. [32] reported a ratiometric FRET-based fluorescent probe for imaging chromium (III) in living cells. A Dansyl-based Cr^{3+} selective fluorescent chemosensor is reported by Wu et al. [33].

On the other hand, coumarin and its derivatives are widely used as anti-coagulants [34], antibacterial agents [35], antifungal agents [36], biological inhibitors [37], chemotherapeutics [38]

* Corresponding author. Tel.: +91 342 2533913; fax: +91 342 2530452.
** Corresponding author.
E-mail address: ddas100in@yahoo.com (D. Das).

0039-9140/$ – see front matter © 2011 Elsevier B.V. All rights reserved.
doi:10.1016/j.talanta.2011.12.014

bio-analytical reagents [39], anti-tumor [40], anti-oxidant [41] cyclooxygenase [42] inhibition.

From the above discussion, it is evident that the use of coumarin derivative as a fluorescent probe for trace level determination of Cr^{3+} and monitoring of intracellular Cr^{3+} in infected cells might be an important area of research. Additionally, use of fluorescence method for chromium speciation is much greener, easier, fast and interesting than the existing conventional techniques. Considering all these facts, herein we report the synthesis, characterizations, speciation and cell imaging studies of a new Cr^{3+} selective fluorescent probe containing coumarin and thiophene units. Our present method is much more superior to our earlier one because it is a fluorescence enhancement method while the earlier one was based on fluorescence quenching. More over the present probe can detect trace level Cr^{3+} in contaminated living cells under fluorescence microscope.

2. Experimental

2.1. Materials

Thiophene-2-carbaldehyde and coumarin have been purchased from Aldrich (USA) and S.D. Fine Chem. Ltd. (India), respectively. 6-Aminocoumarin has been synthesized from coumarin following a literature procedure [43]. Analytical grade chemicals and spectroscopy grade solvents are used. Milli-Q Millipore 18.2 MΩ cm^{-1} water is used throughout all the experiments. Stock solution of Cr(III) (1000 mg L^{-1} in 3% HNO_3) have been obtained from SOLUTIONS Plus Inc. (Missouri, USA) which is tested *vs.* NIST SRM # 3108a. Waste water samples from different sources (three samples from tannery industrial area, Kolkata and three samples from Durgapur Industrial belt, West Bengal, India) are collected for application studies. All the working solutions are prepared by appropriate dilution of the stock solution with de-ionized water. Glass apparatus are kept in 4.0 mol L^{-1} HNO_3 overnight and cleaned with double distilled water. Certified reference materials analyzed were: standard reference material (SRM) 1573 tomato leaves from National Bureau of Standards; pond sediment (NIES 2) and igneous rock (JR-1) from National Institute for Environmental studies, Japan. The sources of Na^+, Ca^{2+}, Mn^{2+}, Cr^{3+}, Fe^{3+}, Co^{2+}, Ni^{2+}, Cu^{2+}, Zn^{2+}, Cd^{2+}, $Hg^{2+}$and Pb^{2+} ions are either their chloride, nitrate or perchlorate salts.

2.2. Instrumentation

^1H NMR spectra are recorded in $CDCl_3$ with a Bruker Advance 300 MHz using tetramethylsilane as the internal standard. Absorption and fluorescence spectra are recorded on Shimadzu Multi Spec 1501 absorption spectrophotometer and Hitachi F-4500 fluorescence spectrophotometer equipped with a temperature controlled cell holder, respectively. Mass spectra are recorded in QTOF Micro YA 263 mass spectrometer in ESI positive mode. IR spectra are recorded on a Perkin Elmer FTIR spectrophotometer (model: RX-1). Micro analytical data (C, H, and N) are collected on Perkin Elmer 2400 CHNS/O elemental analyzer. The fluorescence imaging system is comprised of an inverted fluorescence microscope (Leica DM 1000 LED), digital compact camera (Leica DFC 420C), and an image processor (Leica Application Suite v3.3.0). The microscope is equipped with a mercury 50 W lamp. A domestic Samsung microwave oven (model CE2933) with a 2450 MHz frequency magnetron and 900 W maximum power and a polytetrafluoroethylene (PTFE) reactor (115 mL internal volume, 1 cm cell wall thickness and hermetic screw caps) are used for digestion.

2.3. Synthesis of (6E)-6-((thiophen-2-yl) methyleneamino)-2H-chromen-2-one (**TMC**)

6-Aminocoumarin (0.5 g, 3.1 mmol) and thiophene-2-carboxaldehyde (0.347 g, 3.1 mmol) are taken in dry methanol (15 cm^3) and refluxed for 8 h. After removal of the solvent, a yellow color compound is obtained. Yield 90%; m.p. 138 ± 2 °C; ^1H NMR (300 MHz, $CDCl_3$) (Fig. S1), δ: 6.23 (9.4,d,1H), 6.68 (2.9,d,1H), 7.0 (8.7,d,1H), 7.23 (t,1H), 7.28 (9,d,1H), 7.4 (6,d,1H), 7.49 (s,1H), 7.75 (7.9,d,1H), 9.87 (s,1H). QTOF-MS ES+, (Fig. S2) displays two signals at *m*/*z* 256 and 278, which are assigned as $[M+H]^+$ and $[M+Na]^+$, respectively; FTIR (Fig. S3) (KBr, ν cm^{-1}) ν(CO), 1725; ν(C=N), 1563; UV–vis. spectra (Fig. S4) in CH_3CN–HEPES buffer (4:6, v/v; 0.02 M, pH 7.4) solution at 298 K, λ, nm (ε, 10^3 M^{-1} cm^{-1}), 332 (0.206), 316 (0.195), 278 (0.598), 256 (0.572), 245 (0.587), 219 (0.346). Microanalytical data, calculated for $C_{14}H_9NO_2S$: C, 65.87; H, 3.55; N, 5.49, found: C, 65.88; H, 3.53; N, 5.49.

2.4. Crystal structure determination and refinement of **TMC**

A colorless prism shaped crystal was selected for crystallographic analysis using a BRUKER APPEX-II CCD single crystal X-ray diffractometer. All diffracted intensities were corrected for Lorentz and polarization effects. Absorption correction was performed with Multi-scan BRUKER *SADABS*. The structure was solved by direct methods and was refined by the full-matrix least-squares on F^2 method using SHELXS97 and SHELXL97 computer programs [44]. All the non-hydrogen atoms were refined using anisotropic atomic displacement parameters and hydrogen atoms bonded to carbon were inserted at calculated positions using a riding model. H atoms were placed at idealized positions using standard geometric criteria. The ORTEP program was used to generate the ellipsoid plot and crystal packing diagram was obtained using Mercury software.

2.5. Synthesis of [**TMC**–Cr^{3+}] system

10 mL methanol solution of $Cr(NO_3)_3$, $9H_2O$ (0.025 g, 0.062 mmol) is added slowly to a magnetically stirred 10 mL methanol solution of **TMC** (0.047 g, 0.186 mmol). The mixture is stirred in air for 2 h followed by reflux for 15 min to produce a clear solution. Removal of the solvent yields a deep yellow color complex. QTOF-MS ES^+ (Fig. S5), $[M+H]^+$ = 518; FTIR (Fig. S6) (KBr, ν cm^{-1}): ν(CO), 1724; ν(C=N), 1615 and $\nu(NO_3^-)$, 1385; UV–vis. spectrum (Fig. S4) (in CH_3CN–HEPES buffer, 4:6, v/v, 0.02 M, pH 7.4 at 298 K), λ, nm (ε, 10^3 M^{-1} cm^{-1}): 361 (0.05), 340 (0.045), 265 (0.336), 262 (0.335). Microanalytical data, calculated for $C_{15}H_{19}CrN_3O_{12}S$: C, 34.82; H, 3.70; N, 8.12; found: C, 34.74; H, 3.67; N, 8.1.

2.6. Measurement procedures

Solutions of Cr^{3+} and **TMC** are mixed in different ratios for subsequent fluorescence measurements. The fluorescence emission intensities are measured at 550 nm while the excitation wavelength is fixed at 409 nm. 1.0 cm quartz cell is used for all the measurements.

2.7. Effect of solvent polarity on the emission intensity of **TMC**

Emission intensity of **TMC** was recorded in different solvents having different dielectric constants at room temperature (25 °C).

2.8. Preparation and imaging of cells

To detect intracellular Cr^{3+}, *Candida albicans* cells from exponentially growing culture (in yeast extract glucose broth medium, incubation temperature 37 °C) are centrifuged at 3000 rpm for 10 min and then treated with Cr^{3+} salt (10 μM) for 30 min. After incubation, the cells are washed with normal saline and centrifuged at 3000 rpm for 10 min to remove excess Cr^{3+} which may otherwise interact with the probe and cause background noise. After washing, the cells are treated with **TMC** (10 μM) for 15 min, mounted on a grease free glass slide and observed under high power magnification of a Leica DM 1000 fluorescence microscope with UV filter. Cells without Cr^{3+} treatment but incubated with **TMC** are used as control.

2.9. Effect of *TMC* on the viabilities of cells

Candida cells were collected from 24 h old broth culture through centrifugation (6000 rpm for 5 min). The collected cells were then washed in normal saline and re-suspended in normal saline and then divided into four tubes, (i) Candida control (Candida cells in normal saline), (ii) Candida + Cr(III) salt (in which Candida cells were suspended in normal saline containing 1 mg/mL Cr(III) salt), (iii) Candida + **TMC** (in which Candida cells were suspended in normal saline containing 1 mg/mL **TMC**) and (iv) Candida + Cr(III) salt + **TMC** (in which Candida cells were suspended in normal saline containing both Cr(III) salt and **TMC**).

These four separate tubes were then incubated for 1, 2, 4, 8, 24 h and after each interval, dilution plating was performed using spread plate technique. After incubation at 37 °C, the appeared colonies were counted using an automated bacterial colony counter to check the viability of Candida cells against the Cr(III) salt and **TMC**.

2.10. Estimation of Cr(III) and Cr(VI) from the binary synthetic mixtures and real samples

Different amounts of Cr(III) and Cr(VI) were mixed in different sets (each set in duplicate) in a total volume of 100 mL. Direct estimation of Cr(III) was performed using our developed method. Reduction of Cr(VI) to Cr(III) by equivalent amount of oxalic acid was performed and total Cr(III) in the solution was estimated as mentioned above. The difference gave free Cr(VI) present in the solution.

The waste water samples from different sources (three samples from tannery industrial area, Kolkata and three samples from Durgapur Industrial belt, West Bengal, India) were filtered through a 0.45 μm Milipore membrane filter and analyzed as per our developed method.

3. Results and discussion

3.1. Spectral and structural characteristics

Scheme 1 shows the facile one step synthesis of the **TMC**. Crystal data and structure refinement for **TMC** is presented in Table 1. Crystal packing diagram and ORTEP view of **TMC** is presented in Fig. 1. Fig. S4 illustrates the UV–vis. titration of **TMC** with externally added Cr^{3+} at 25 °C in CH_3CN–HEPES buffer (4:6, v/v, 0.02 M, pH 7.4). The absorbance of **TMC** at 260 nm gradually increases with increasing [Cr^{3+}]. Distinct differential nature of UV–vis. spectra of **TMC**–Cr^{3+} complex to that of **TMC** indicates the formation of **TMC**–Cr^{3+} complex. Inset plot shows the expanded region from 250 nm to 400 nm.

Fig. 2 reveals that acetonitrile is the most useful solvent over other common solvents *viz.* methanol, ethanol, *N*,*N*-dimethylformamide (DMF), dimethyl sulfoxide (DMSO), chloroform and dichloromethane (DCM). The solvent dependency of

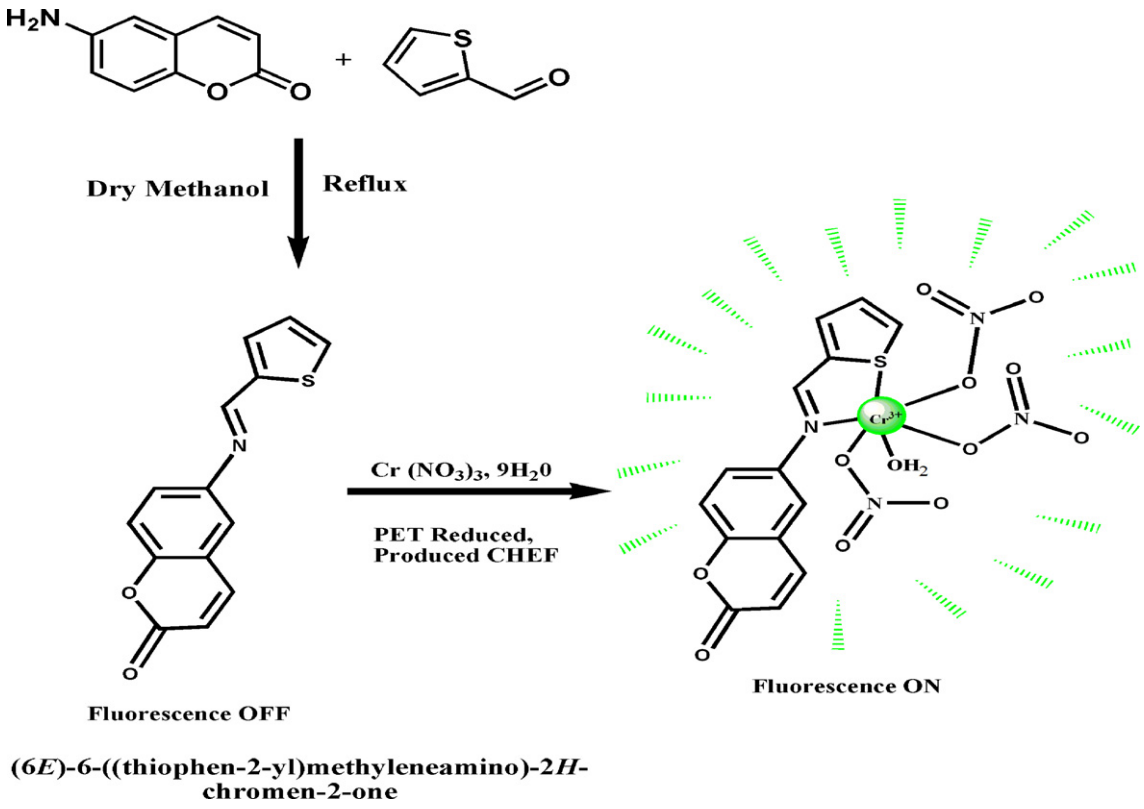

Scheme 1. Synthesis of fluorescent sensor of (6E)-6-((thiophen-2-yl) methyleneamino)-2H-chromen-2-one (**TMC**).

Table 1
Crystal data and structure refinement for **TMC**.

Crystal formula	$C_{14}H_9NO_2S$
Formula weight	255.28
Temp (K)	100 K
Mo $K\alpha$ radiation, λ=	0.7107 Å
Crystal system	Orthorhombic
Crystal shape and color	Prism, colorless
Crystal dimension	0.17 mm × 0.12 mm × 0.09 mm
Density	1.474 mg m^{-3}
θ_{max}=	26.4°
θ_{min}=	1.5°
Space group	$Pca2_1$
a (Å)	6.950(2)
b (Å)	6.1751(17)
c (Å)	26.797(9)
V (Å^3)	1150.05
Z	4
$R[F2 > 2\sigma(F2)]$=	0.037
$wR(F2)$=	0.086
h, k and l=	0 → 8, 0 → 7, −33 → 33

$w = 1/[\sigma 2(Fo^2) + (0.0412P)^2 + 0.2648P]$ where $P = (Fo^2 + 2Fc^2)/3$.

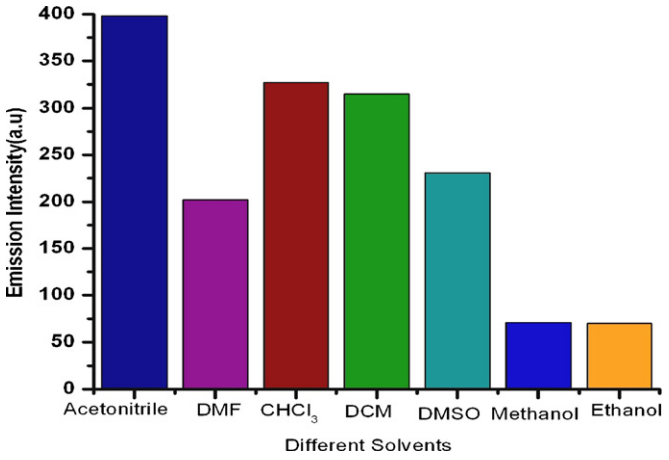

Fig. 2. Emission intensities of **TMC** (10 μM) in different solvents (λ_{ex} = 409 nm, λ_{em} = 550 nm, slit width, 10/10).

the fluorescence intensity suggests that the solvent molecule plays an important role to the emission process. A plot of fluorescence intensity of **TMC** as a function of dielectric constant of the solvent is shown in Fig. 3 which shows an increase in the emission intensity of **TMC** with more polar solvent indicating stabilization of the fluorescence excited state of **TMC** in polar media [45]. Addition of Cr^{3+} to the solution of **TMC** results the enhancement of fluorescence intensity at 550 nm (λ_{ex} = 409 nm). Changes in the emission intensities of **TMC** as a function of externally added [Cr^{3+}] (0.1–6 μM) are presented in Fig. 4.

Fluorescence quantum yield of the [**TMC** + Cr(III)] system is almost 5 times (0.575) than that of free **TMC** (0.118) [ESI].

Job's plot (Fig. 5) indicates a 1:1 stoichiometry of the complex formed between **TMC** and Cr^{3+}, which is also supported by the mass spectra of Cr^{3+}–**TMC** complex. Chelation of **TMC** with Cr^{3+} makes the lone pair of electrons on nitrogen of the imine function unavailable for PET [46]. Chelation also increased the rigidity of the complex molecule by restricting the free rotation of the thiophene ring around the azomethine function. Combination of two effects have resulted the enhancement of the fluorescence intensity of the complex in comparison to free **TMC**. Thus, the system behaves like an "OFF–ON" switch.

3.2. Estimation of binding constant

The binding ability of **TMC** towards Cr^{3+} has been estimated following the modified Benesi–Hildebrand equation (Fig. 6) [47].

$$\left(\frac{1}{\Delta F}\right) = \frac{1}{\Delta F_{max}} + \left(\frac{1}{K[C]^n}\right)\left(\frac{1}{\Delta F_{max}}\right).$$

where $\Delta F = (F_x - F_0)$ and $\Delta F_{max} = F_\infty - F_0$, where F_0, F_x, and F_∞ are the emission intensities of **TMC** in the absence of Cr^{3+}, at an intermediate Cr^{3+} concentration, and at the concentration of complete

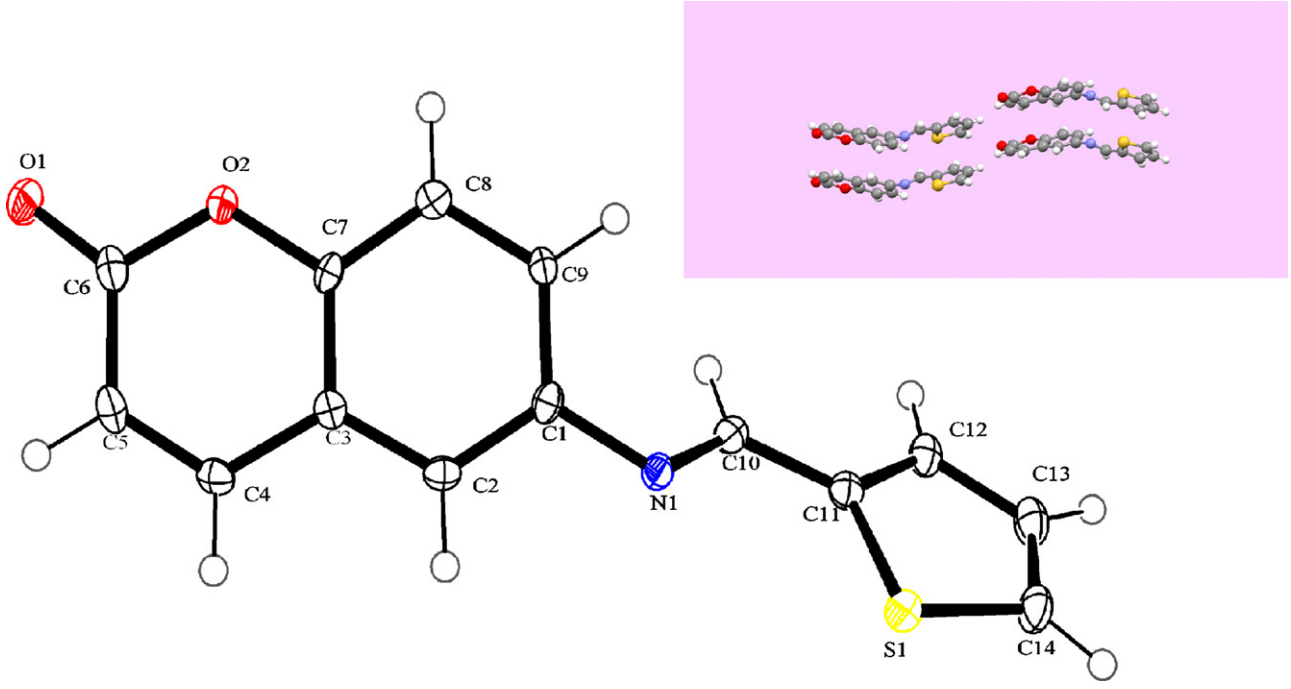

Fig. 1. Single crystal X-ray structure and packing diagram (inset) of **TMC**.

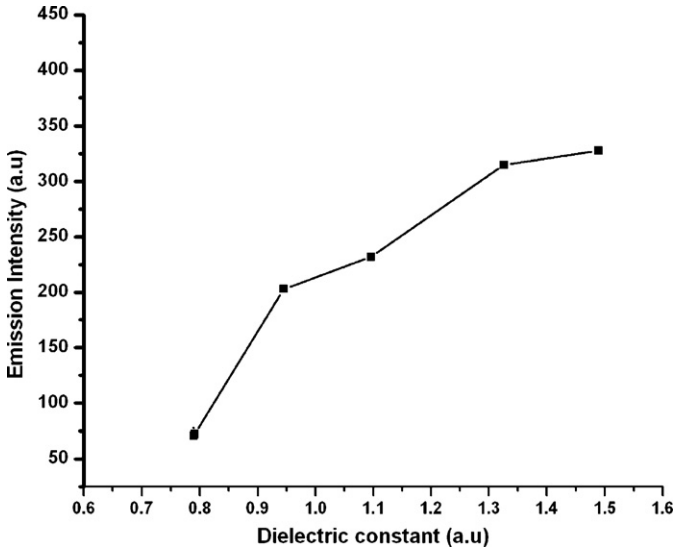

Fig. 3. Variation of emission intensity of **TMC** as a function of dielectric constant of solvents.

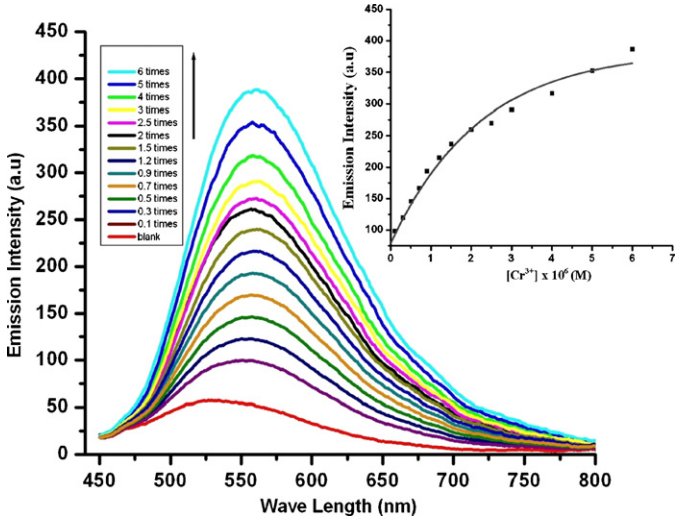

Fig. 4. Fluorescence spectral changes of **TMC** (10 μM) up on addition of 0.5, 1, 1.5, 2, 2.5, 3, 4, 5, 6, 7, 8, 9, 10 μM of Cr^{3+} ion.

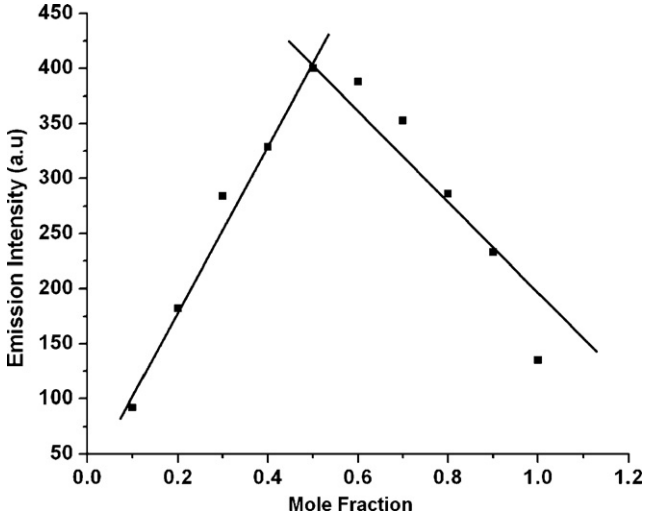

Fig. 5. Jobs plot for the determination of stoichiometry of [**TMC**–Cr^{3+}] in solution.

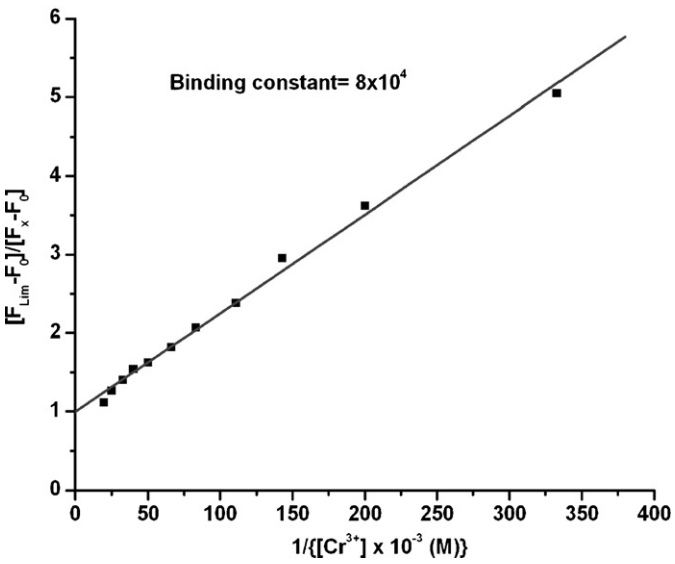

Fig. 6. Determination of binding constant of **TMC** (10 μM) with Cr^{3+} (10 μM) using Benesi–Hildebrand equation (fluorescence method).

interaction, respectively. *K* is the binding constant and *C* is the Cr^{3+} concentration and *n* is the number of Cr^{3+} ion bound per **TMC** (here, $n = 1$). The value of *K* obtained from the slope is 8×10^4.

TMC could detect as low as 0.1 μM Cr^{3+} in CH_3CN–HEPES buffer (4:6, v/v, 0.02 M, pH 7.4). Fig. 7 shows the plot of emission intensities of **TMC** as a function of externally added [Cr^{3+}], which can be used for the determination of unknown [Cr^{3+}] in a sample. Up to 2 times (2 μM) of the externally added Cr^{3+} ion, we observed linearity.

3.3. Selectivity

The selectivity of **TMC** for Cr^{3+} over other common metal ions at biologically concentration level is examined in CH_3CN–HEPES buffer (4:6, v/v, 0.02 M, pH 7.4). Fig. 8 indicates that only Cr^{3+} enhances the fluorescence intensity of **TMC** whereas other 3d metal ions, except Fe^{3+} and Cu^{2+} (which quenches the emission intensity of **TMC** to some extent) have no significant effect on the emission intensity of **TMC**. Inset of Fig. 8 shows the picture of free

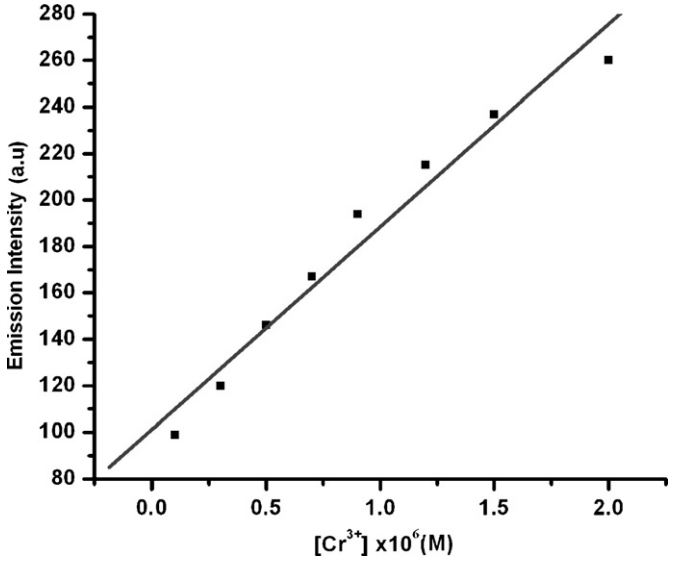

Fig. 7. Plot of emission intensities of **TMC** (10 μM) as a function of externally added [Cr^{3+}].

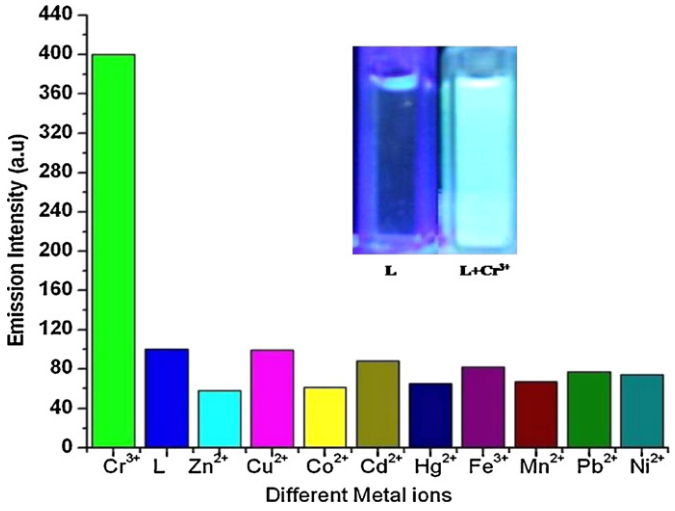

Fig. 8. Emission intensities of **TMC** (10 μM) in presence of different metal ions (10 μM).

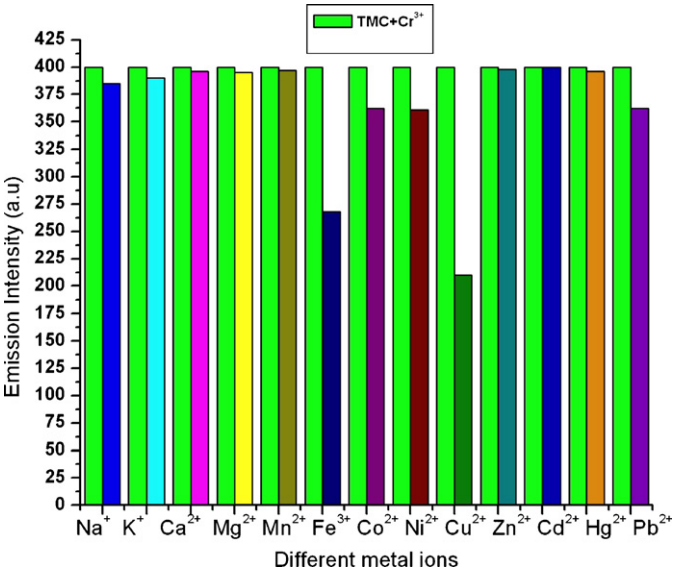

Fig. 9. Interference of different metal ions on the determination of $[Cr^{3+}]$ using **TMC**. $[\mathbf{TMC}] = [Cr^{3+}] = 10\ \mu M$, [foreign metal ions] = 1×10^{-6} M.

TMC solution (10 μM) and after addition of 1.0 equivalent Cr^{3+} under a hand held UV lamp.

Fig. 9 shows the effect of common alkali, alkaline earth and transition metal ions on the emission intensity of the [**TMC**–Cr^{3+}] system. Except Fe^{3+} and Cu^{2+} ions, no other metal ions interfered significantly. Effect of Fe^{3+} and Cu^{2+} ions has been eliminated using thiocyanate as a masking agent which have no effect on the emission properties of the [**TMC**–Cr^{3+}] system. Common accompanying anions have no effect on the emission intensity of [**TMC**–Cr^{3+}] system as evident from Fig. 10.

4. Speciation studies

So far we have observed that Cr(III) can enhance the fluorescence intensity of the **TMC** significantly and we can detect and estimate trace level Cr(III) in aqueous solution. But Cr(VI) has no effect on the fluorescence intensity of the **TMC**. So we converted Cr(VI) to Cr(III) by using two different reducing agents, *viz.* oxalic acid and sodium dithionite. In our case oxalic acid worked

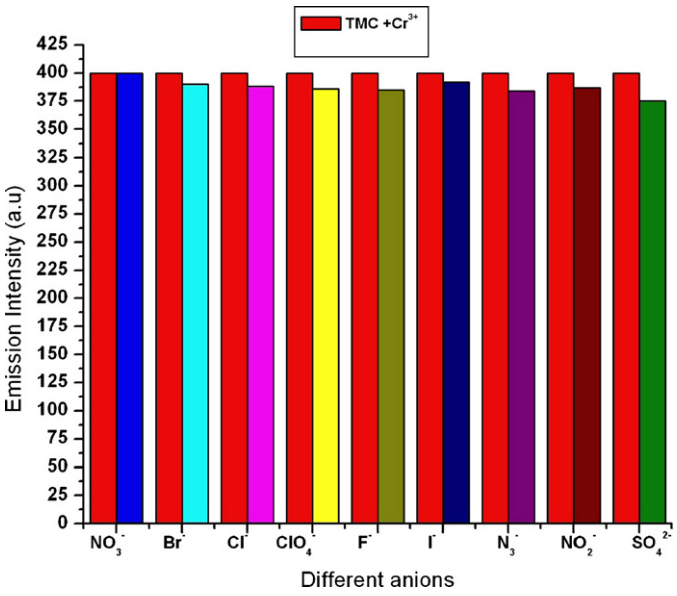

Fig. 10. Interference of different anions on the determination of $[Cr^{3+}]$ with **TMC**. $[\mathbf{TMC}] = [Cr^{3+}] = [\text{foreign anions}] = 10\ \mu M$.

better. We have already mentioned that oxalate or dithionate and dithionite have no adverse effect on the emission intensities of either free ligand or **TMC**–Cr(III) complex. So, slight excess of these species in the mixture will not be harmful to our methodology. Only thing, we have to do after oxalic acid assisted reduction of Cr(VI) to Cr(III), the pH of the medium should be neutral. Fig. 11 shows the changes of the fluorescence emission intensities of **TMC** (1×10^{-6} mol L^{-1}) with the addition of different concentrations of Cr(VI) (1×10^{-6}–6×10^{-6} mol L^{-1}) followed by equivalent amount of oxalic acid. It can be said that with increasing [Cr(VI)], proportionate amount of [Cr(III)] produced *in situ* which reacted with the **TMC** and consequently, emission intensities of the system increased gradually. Thus, in a mixture of Cr(III) and Cr(VI), we can directly measure free [Cr(III)] and total [Cr(III)] (which is sum of free Cr(III) and Cr(III) produced from free Cr(VI) after reduction with oxalic acid). Difference will give free [Cr(VI)].

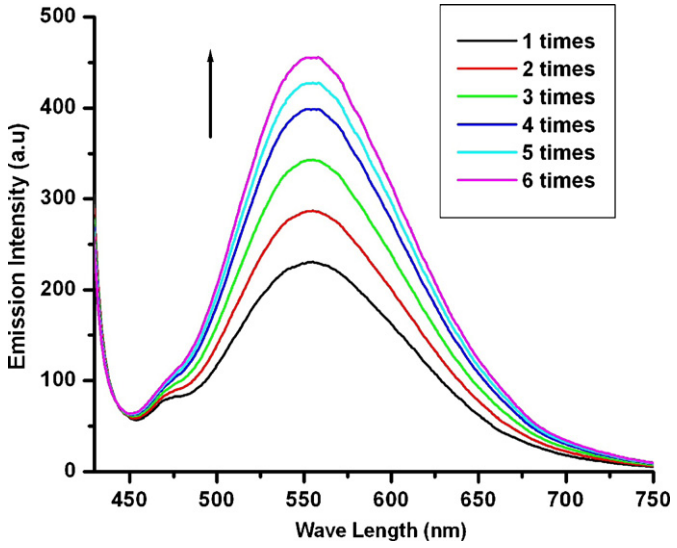

Fig. 11. Changes of the fluorescence intensities of **TMC** (1 μM) in aqueous solutions as a function of converted $[Cr^{3+}]$, obtained by the reduction of Cr(VI) at neutral P^H.

Table 2
Determination of Cr(III) and Cr(VI) in synthetic binary synthetic mixtures.

No. of observations	Amount taken (μg)	Amount found (μg)	Error (%)
1	Cr(III) – 50	Cr(III) – 48.9 ± 0.6	1.1
	Cr(VI) -50	Cr(VI) – 49.4 ± 0.06	0.6
2	Cr(III) – 40	Cr(III) – 38.6 ± 0.5	1.4
	Cr(VI) – 50	Cr(VI) – 48.5 ± 0.6	1.5
3	Cr(III) – 65	Cr(III) – 64.1 ± 0.03	0.9
	Cr(VI) – 25	Cr(VI) – 26.2 ± 0.09	1.2
4	Cr(III) – 30	Cr(III) – 31.3 ± 0.5	1.3
	Cr(VI) – 45	Cr(VI) – 44.2 ± 0.7	0.8
5	Cr(III) – 30	Cr(III) – 29.1 ± 0.5	0.9
	Cr(VI) – 40	Cr(VI) – 40.4 ± 0.7	0.4

Table 3
Determination of chromium species in environmental samples.

Sample no.	Present method		Reference method [18]	
	Cr(III)	Cr(VI)	Cr(III)	Cr(VI)
1[a]	681.2 ± 0.2	595 ± 2	683.2 ± 0.2	595.9 ± 2
2[a]	575 ± 3	512 ± 4	571.6 ± 3	511.2 ± 4
3[a]	467 ± 1	415 ± 3	475 ± 1	417.2 ± 3
4[b]	65.3 ± 3	54.5 ± 1	63.3 ± 3	52.5 ± 1
5[b]	43.1 ± 3	41.2 ± 4	43.8 ± 3	44.2 ± 4
6[b]	35.5 ± 4	37.5 ± 5	35.8 ± 4	34.5 ± 5

[a] Tannery water.
[b] Industrial water.

5. Cell imaging

From Fig. 12, we could conclude that Fluorescence microscope images of *Candida albicans* cells (IMTECH No. 3018): (a) only Cr^{3+} pre-treated cells had been stained by **TMC** (b) **TMC** was easily permeable through the cell membrane without causing any harm as the cells remain alive even after 30 min of exposure to **TMC** at 10 μM under 100× objective lens. Incubation was performed at 37 °C.

The photographs indicate that the ligand can be used to detect the presence of intracellular Cr^{3+} in living cells. The ligand may be useful for detecting presence of Cr^{3+} in any type of natural sample from the suspected spot having any kind of living cells such as bacteria, fungi and protozoa.

Table 4
Comparison of the present method with other Cr(III) selective turn-on fluorescence sensors.

Sensor type	Selectivity	LOD	Association constant	Application	Interferences	Ref.
Turn off	Only Cr(III) in DMF:water (9:1, v/v)	9×10^{-6} mol L^{-1}	8.1378×10^4 M^{-1}	–	Na^+, K^+, Mg^{2+}, Ca^{2+}, Cd^{2+}, Zn^{2+}, Hg^{2+}, Mn^{2+}, Cu^{2+}, Fe^{3+}, Co^{2+}, Pb^{2+}, Ni^{2+} show insignificant positive interferences	[28]
Turn on	Fe(III) and Cr(III) in aqueous solution	–	41,600 M^{-1}	–	Co^{2+}, Ni^{2+}, Zn^{2+}, Cd^{2+}, Ag^+, Pb^{2+}, Ba^{2+}, Mg^{2+}, Ca^{2+}, K^+ and Na^+ displayed little interference	[30]
Turn on	Only Cr(III) in ethanol/H_2O (1:1, v/v, pH 7.4)	–	$K_a = 7.5 \times 10^3$ M^{-1}	Cell imaging	Only Hg^{2+} enhanced fluorescence intensity to a small extent	[31]
FRET-based ratiometric	Only Cr(III) in ethanol–water (2:1, v/v)	–	$K_a = 9.4 \times 10^3$ M^{-1}	Cell imaging	Zn^{2+}, Cu^{2+}, Fe^{2+}, Mn^{2+}, Co^{2+}, Ni^{2+}, Cd^{2+}, Hg^{2+}, Ag^+, Pb^{2+} provided weak interferences	[32]
Turn on	Only Cr(III) in (DMF/H2O = 9:1, v/v)	–	$K_{ass} = 6.07 \pm 0.10 \times 10^7$ M^{-2}	–	Mg^{2+}, Ca^{2+} and Mn^{2+}, increased the fluorescence to a slight extent while the presence of 0.2 mM Zn^{2+}, Cd^{2+}, Fe^{3+}, Hg^{2+} and Pb^{2+} quenched the fluorescence to a slight extent	[33]
Turn on	Only Cr(III) in aqueous media	1.6×10^{-8} M	–	–	No interference from other metal ions	[48]
Turn on	Only Cr(III) in acetonitrile–water (1:1, v/v)	2.5 μg l^{-1}	$K = 4.7 \times 10^5$ l mol^{-1}	Domestic and industrial waste water analysis	No interference	[49]
Turn on	Only Cr(III) in CH_3CN–HEPES buffer (4:6, v/v, 0.02 M)	1×10^{-6} M.	$K_a = 8 \times 10^4$ M^{-1}	Cell imaging	Fe^{3+} and Cu^{2+} interfered to some extent while Co^{2+}, Ni^{2+} and Pb^{2+} interfered to a negligible extent	Present

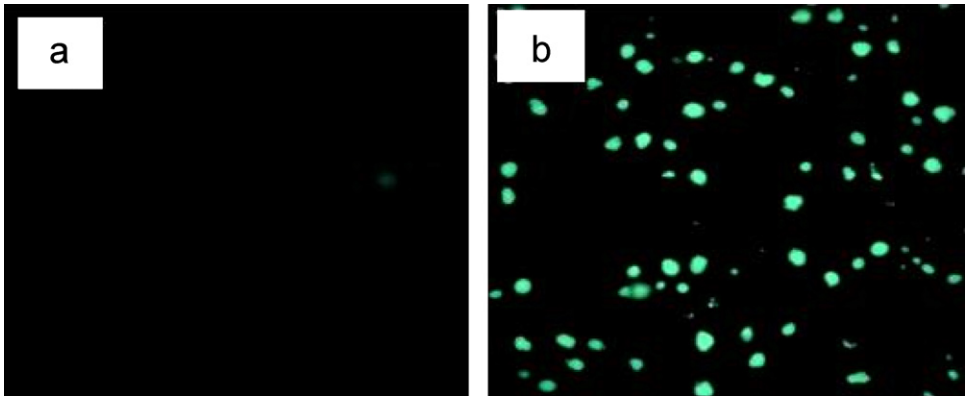

Fig. 12. Fluorescence microscope images of *Candida albicans* cells (IMTECH No. 3018): (a) image of *Candida albicans* without treatment with **TMC** (b) Fluorescence image of **TMC** stained *Candida albicans* cells exposed to (10 μM) Cr^{3+} for 30 min under 100X objective lens. Incubation was performed at 37 °C.

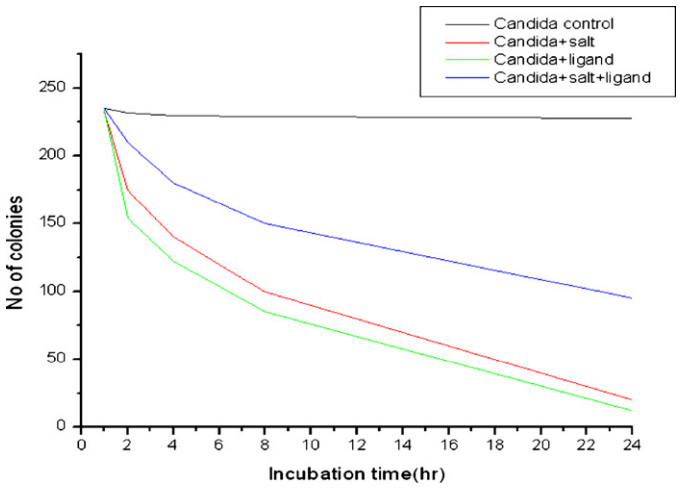

Fig. 13. Effect of **TMC** on the viabilities of cells.

6. Cell viability assay

It is interesting to note from Fig. 13 that cells loaded with both **TMC** and Cr(III) salt have longer life time than those treated with only **TMC** or Cr(III) salt. 80% cells remain alive even after 8 h of treatment with **TMC** and Cr(III) salt together.

7. Applications

Table 2 shows that a fair degree of agreement between the observed results and true values. In case of real samples analysis, the results were in good agreement (t-test, $P = 0.06$) with a reference method [18] (Table 3).

8. Conclusion

Coumarin based fluorescent sensor, **TMC** can detect Cr^{3+} in acetonitrile–HEPES buffer medium. **TMC** is successfully used for trace level Cr^{3+} detection in living cells under the fluorescence microscope. Cr^{3+} assisted fluorescence enhancement of **TMC** is attributed to the inhibition of PET and restricted rotation around the imine bond of the molecule. Small interference from Fe^{3+} and Cu^{2+} was masked using thiocyanate. Speciation studies have been performed in a very lucid, fast and green way. This new Cr^{3+} selective fluorescent probe may find potential bio-medical applications. This fact helped us in Cr speciation without any cumbersome pre-separation process. Analysis of Cr species in different synthetic as well as environmental samples has been successfully performed. Comparison of the present method with some other existing Cr(III) sensitive turn-on fluorescent probes (Table 4) clearly indicates the superiority of our method. Amongst the reported fluorescent probes, only the probe developed by Mao et al. [48] has better LOD. Tang et al. [49] have reported stronger binding constant of their probe with Cr(III). Our probe is least expensive as it involves a facile one step reaction with commercially available much cheaper chemicals. Moreover, they did not report cell imaging property of the probe.

Acknowledgements

Financial support from UGC-DAE-Kolkata center and West Bengal state DST is gratefully acknowledged. We convey our sincere thanks to USIC, Burdwan University for extending the facility of fluorescence microscope.

Appendix A. Supplementary data

CCDC 855223 contains the structural details of the probe **TMC**.

Supplementary data associated with this article can be found, in the online version, at doi:10.1016/j.talanta.2011.12.014.

References

[1] V. Gómez, M.P. Callao, Trends Anal. Chem. 25 (2006) 1006.
[2] R.D. Mount, J.R. Hockett, Water Res. 34 (2000) 1379.
[3] H.F. Maltez, E. Carasek, Talanta 65 (2005) 537.
[4] S.A. Katz, H. Salem, The Biological and Environmental Chemistry of Chromium, VCH Publishers, New York, 1994.
[5] J. de Silva, R. Williams, The Biological Chemistry of the Elements, Inorganic Chemistry of Life, Clarendon Press, Oxford, NY, 1991, pp. 541–543.
[6] R. Murphy, J. Guertin, J.A. Jacobs, C.P. Avakian (Eds.), Chromium (VI) Handbook, CRC Press, New York, 2004, p. 593.
[7] N.H. Furman, F.J. Welcher, W.W. Scott, Standard Methods of Chemical Analysis V1, Van Nostrand, 1962.
[8] S.S.M. Hassan, M.N. Abbas, G.A.E. Moustafa, Talanta 43 (1996) 797.
[9] M.A. Zayed, B.N. Barsoum, A.E. Hassan, Microchem. J. 54 (1996) 72.
[10] N. Balasubramanian, V. Maheswari, J. AOAC Int. 79 (1996) 989.
[11] V. Maheswari, N. Balasubramanian, Chem. Anal. (Warsaw) 41 (1996) 569.
[12] N. Jie, J. Jiang, Analyst 116 (1991) 395.
[13] J. Yang, J. Guo, Anal. Lett. 25 (1992) 1447.
[14] E.J. Arar, J.O. Pfaff, J. Chromatogr. 546 (1991) 335.
[15] V. Ososkov, B. Kebbekus, D. Chesbro, Anal. Lett. 29 (1996) 1829.
[16] B. Demirata, Mikrochim. Acta 136 (2001) 143.
[17] A. Tunceli, A.R. Turker, Talanta 57 (2002) 1199.
[18] A. Xue, S. Qian, G. Huang, L. Chen, J. Anal. Spectrom. 15 (2000) 1513.
[19] F. Shemirani, M. Rajabi, Fresenius J. Anal. Chem. 371 (2001) 1037.
[20] M. Sugiyaura, O. Fujino, S. Kihara, M. Matsui, Anal. Chim. Acta 181 (1986) 159.
[21] S. Peräniemi, M. Ahlgré, Anal. Chim. Acta 315 (1995) 365.
[22] I. Turyan, D. Mandler, Anal. Chem. 69 (1997) 894.
[23] D.V. Vukomanovic, G.V. Vanloon, K. Nakatsu, D.E. zoutman, Microchem. J. 57 (1997) 86.
[24] K. Yoshimura, Analyst 113 (1988) 471.
[25] K.O. Saygi, J. Hazard. Mater. 153 (2008) 1009.
[26] Q. Wan, Y. Guo, X. Wang, A. Xia, Anal. Chim. Acta 665 (2010) 215.
[27] V. Kabasakalis, Anal. Lett. 26 (1993) 2269.
[28] D. Karak, A. Banerjee, A. Sahana, S. Guha, S. Lohar, S. Sekhar Adhikari, D. Das, J. Hazard. Mater. 188 (2011) 274.
[29] M. Sarkar, S. Banthia, A. Samanta, Tetrahedron Lett. 43 (2006) 7575.
[30] J. Mao, L.N. Wang, W. Dou, X.L. Tang, Y. Yan, W.S. Liu, Org. Lett. 9 (2007) 3188.
[31] K. Huang, H. Yang, Z. Zhou, M. Yu, F. Li, X. Gao, T. Yi, C. Huang, Org. Lett. 10 (2008) 2557.
[32] Z. Zhou, M. Yu, H. Yang, K. Huang, F. Li, T. Yi, C. Huang, Chem. Commun. (2008) 3387.
[33] H. Wu, P. Zhou, J. Wang, L. Zhao, C. Duan, New J. Chem. 33 (2009) 653.
[34] J.W. Suttie, Clin. Cardiol. 13 (1990) 16.
[35] A.A.A. Abu-Hussein, J. Coord. Chem. 59 (2006) 157.
[36] T. Patonay, G. Litkei, R. Bognar, J. Eredi, C. Miszti, Pharmazie 39 (1984) 86.
[37] C. Gnerre, M. Catto, F. Leonetti, P. Weber, P.A. Carrupt, C. Altomare, A. Carotti, B. Testa, J. Med. Chem. 43 (2000) 4747.
[38] E. Budzisz, B.K. Keppler, G. Giester, M. Wozniczka, A. Kufelnicki, B. Nawrot, J. Inorg. Chem. 22 (2004) 4412.
[39] M. Jiménez, J.J. Mateo, R. Mateo, J. Chromatogr. A 870 (2000) 473.
[40] D. Egan, R. O'Kennedy, E. Moran, D. Cox, E. Prosser, R.D. Thornes, Drug Metab. Rev. 22 (1990) 503–529.
[41] R.N. Gacche, D.S. Gond, N.A. Dhole, B.S. Dawane, J. Enzyme Inhib. Med. Chem. 21 (2006) 157.
[42] Y. Kimura, H. Okuda, S. Arichi, K. Baba, M. Kozawa, Biochim. Biophys. Acta 834 (1985) 224.
[43] S. Roy, T.K. Mondal, P. Mitra, E.L. Torres, C. Sinha, Polyhedron 30 (2011) 913.
[44] G.M. Sheldrick, Acta Crystallogr. A 64 (2008) 112–122.
[45] D. Ray, P.K. Bharadwaj, Inorg. Chem. 47 (2008) 2252.
[46] J.R. Lakowicz, Principles of Fluorescence Spectroscopy, third ed., Springer, New York, 2006.
[47] H.A. Benesi, J.H. Hildebrand, J. Am. Chem. Soc. 71 (1947) 2703.
[48] J. Mao, Q. He, W. Liu, Anal. Bioanal. Chem. 396 (2010) 1197.
[49] B. Tang, T. Yue, J. Wu, Y. Dong, Y. Ding, H. Wang, Talanta 64 (2004) 955.